Quality parameters analysis of optical imaging systems with enhanced focal depth using the Wigner distribution function

Dobryna Zalvidea, Cecilia Colautti, and Enrique E. Sicre

Centro de Investigaciones Opticas, P.O. Box 124, 1900 La Plata, Argentina

Received July 12, 1999; revised manuscript received January 10, 2000; accepted January 21, 2000

An analysis of the Strehl ratio and the optical transfer function as imaging quality parameters of optical elements with enhanced focal length is carried out by employing the Wigner distribution function. To this end, we use four different pupil functions: a full circular aperture, a hyper-Gaussian aperture, a quartic phase plate, and a logarithmic phase mask. A comparison is performed between the quality parameters and test images formed by these pupil functions at different defocus distances. © 2000 Optical Society of America [S0740-3232(00)00605-0]

OCIS codes: 100.5070, 110.4850, 110.5100.

1. INTRODUCTION

In recent years several types of optical elements that give rise to well-focused energy distributions along three-dimensional paths have been extensively reported in the literature (see, e.g., Ref. 1). Annular-type apertures acting as apodizers to improve the quality of the point-spread function (PSF) and to increase the focal depth have been studied.[2–8] However, the main drawback of all these methods arises from the fact that both the spatial resolution and the optical power decrease at the image plane. An alternative way to achieve an extended depth of field without using apodizers was reported by Häusler[9] for the case in which focusing can be varied through the image-forming process. In this way, the image field is adequately scanned to produce a well-focused PSF at each image point. Another type of optical system that allows the concentration of energy in a segment of the optical axis is the so-called axilens; such lenses have an associated focal length that varies with the radial coordinate, so their phase retardation functions differ from those of the conventional quadratic phase exponential.[10,11] Therefore, if these phase masks are employed as pupil functions of an imaging optical system, although there is no decrease in the image intensity the resulting PSF becomes relatively broad.

To evaluate the image quality originated by an optical system with a required focal depth, it seems adequate to use different parameters: for example, the Strehl ratio[12] (SR), which gives information about the energy concentration along the optical axis, and the optical transfer function (OTF), which shows the behavior of the optical system for varying spatial frequencies.[13] There are several criteria for specifying the tolerance of an optical system to aberrations or focus error, for example, Rayleigh's criterion,[14] and Marechal's treatment of tolerances.[15] In all these criteria the on-axis image irradiance is the relevant quantity. Hopkins[16,17] has shown that it is possible to extend Marechal's treatment by employing OTF theory to give a tolerance criterion. This method is quite suitable as a merit function in automatic optical design.

The relationships between these image quality criteria and the phase-space representations, namely, the Wigner distribution function[18,19] (WDF) and the ambiguity function,[20] (AF) were employed in several studies to analyze the performance of an optical system with respect to different aberrations and defocus.[21–26]

In a previous paper[27] we proposed a method for obtaining phase retardation functions that give rise to an increase in the image focal depth. To this end, the WDF of a certain aperture with small depth of focus in the image space is sheared in the phase-space domain to originate a new WDF from which its related phase pupil gives rise to a more uniform on-axis image irradiance. In this way, a new phase pupil function with a good performance with respect to defocus, is obtained. A lens axicon with a similar phase function was also proposed by Jaroszewicz and Morales,[28] with use of geometrical optics.

In the present paper we first briefly describe the phase-space formalism and its relationships to different image-quality parameters. In particular, an expression of the SR as a function of the WDF of a bidimensional radially symmetric aperture is obtained for any out-of-focus plane. Then we extend the approach to analyze the relationship between the OTF of this kind of pupil function and the related WDF. We apply this analysis to study the behavior of different phase and amplitude pupil functions[7,11] at various defocus distances.

2. WIGNER DISTRIBUTION FUNCTION: DEFINITIONS AND BASIC RELATIONSHIPS

For a two-dimensional complex-valued function $g(x, y)$, its associated WDF phase-space representation can be alternatively defined from the function itself or from its spectrum $\tilde{G}(\nu, \mu)$ as

0740-3232/2000/050867-07$15.00

$$W_g(x, y; \nu, \mu) = \int\int_{-\infty}^{+\infty} g\left(x + \frac{x'}{2}, y + \frac{y'}{2}\right) \times g^*\left(x - \frac{x'}{2}, y - \frac{y'}{2}\right) \times \exp[-2\pi i(x'\nu + y'\mu)]dx'dy' = \int\int_{-\infty}^{+\infty} \tilde{G}\left(\nu + \frac{\nu'}{2}, \mu + \frac{\mu'}{2}\right) \times \tilde{G}^*\left(\nu - \frac{\nu'}{2}, \mu - \frac{\mu'}{2}\right) \times \exp[2\pi i(x\nu' + y\mu')]d\nu'd\mu', \quad (1)$$

respectively. From Eq. (1) it can be deduced that this formalism emphasizes equally the role of the spatial and the spatial-frequency coordinates. This feature makes these distributions especially suitable for describing the behavior of optical imaging systems. Among several properties of these distributions, those that are relevant for analyzing image-quality parameters are the following:

$$W_z(x, y; \nu, \mu) = W_0(x - \lambda z\nu, y - \lambda z\mu; \nu, \mu), \quad (2)$$

$$I(x, y; z) = \int\int_{-\infty}^{\infty} W_z(x, y; \nu, \mu)d\nu d\mu, \quad (3)$$

$$t(x, y) = \frac{1}{t^*(0, 0)} \int\int_{-\infty}^{\infty} W_t\left(\frac{x}{2}, \frac{y}{2}; \nu, \mu\right) \times \exp[2\pi i(\nu x + \mu y)]d\nu d\mu. \quad (4)$$

Equation (2) states that, under free-space propagation in the Fresnel diffraction region, the WDF associated with the light field is sheared in the phase space only along the spatial coordinates. In Eq. (3) the intensity distribution at a certain plane is found by projecting the WDF onto the spatial-frequency plane. The Fourier transform in Eq. (4) allows recovery of the signal from the WDF.

3. IMAGE-QUALITY PARAMETERS AND THE WIGNER DISTRIBUTION FUNCTION: BASIC THEORY

Let us consider an optical imaging system that can be described by the amplitude PSF. At the image plane ($z = 0$), the PSF is given through a Fourier transform relationship

$$p(x, y; z = 0) = \frac{A}{\lambda f}\exp\left[i\frac{\pi}{\lambda f}(x^2 + y^2)\right] \times \int\int_{-\infty}^{\infty} t(\xi, \eta)\exp\left[-\frac{2\pi i}{\lambda f}(x\xi + y\eta)\right] \times d\xi d\eta, \quad (5)$$

where A is the constant incident amplitude, f is the focal length, and $t(\xi, \eta)$ is the complex-amplitude transmittance associated with the exit pupil. By taking into account the WDF definition as given by Eq. (1) and replacing $p(x, y)$, as given by Eq. (5), we find the WDF at the image plane to be

$$W_i(x, y; \nu, \mu) = (\lambda f)^2 W_t\left(x - \lambda f\nu, y - \lambda f\mu; \frac{x}{\lambda f}, \frac{y}{\lambda f}\right), \quad (6)$$

where $W_t(x, y; \nu, \mu)$ is the WDF of the pupil function $t(\xi, \eta)$. Accordingly, with Eqs. (2) and (3), the intensity at a defocused plane ($z \neq 0$) can be found as

$$I(x, y; z) = \int\int_{-\infty}^{\infty} W_i(x - \lambda z\nu, y - \lambda z\mu; \nu, \mu)d\nu d\mu = (\lambda f)^2 \int\int_{-\infty}^{\infty} d\nu d\mu W_t\left[x - \lambda(f + z)\nu, y - \lambda(f + z)\mu; \frac{x}{\lambda f} - \frac{z}{f}\nu, \frac{y}{\lambda f} - \frac{z}{f}\mu\right]. \quad (7)$$

From Eq. (7), the Strehl ratio versus defocus $S(z)$ can be easily derived as

$$S(z) = \frac{I(0, 0; z)}{I(0, 0; 0)} = K\int\int_{-\infty}^{\infty} d\zeta_1 d\zeta_2 \times W_t(x - \lambda(f + z)\zeta_1, y - \lambda(f + z)\zeta_2; \zeta_1, \zeta_2), \quad (8)$$

where $\zeta_1 = (-z/f)\nu$, $\zeta_2 = (-z/f)\mu$ are redefined spatial frequencies, and $K = (\lambda f^2/za)^2$, a being the pupil area. Thus, the behavior of the optical imaging system can be visualized through the spatial variation of the function $S(z)$, which in turn is obtained from the summation of the values of $W_t(x, y; \nu, \mu)$ along different lines in the phase space. However, although Eq. (8) provides a complete description of the SR for any plane $z \neq 0$, it involves the manipulation of a function defined in a four-dimensional phase space. If we restrict the analysis to radially symmetric apertures, i.e., $t(\xi, \eta) = t(\rho)$, where $\rho = (\xi^2 + \eta^2)^{1/2}$, then the information content of the phase space $(x, y; \zeta_1, \zeta_2)$ [from which the SR, $S(z)$, is obtained] can be displayed in a modified two-dimensional phase space (x, ζ). To this end, we rewrite the intensity in the neighborhood of the image plane as

$$I(x, y; z) = |p(x, y; z|^2. \quad (9)$$

Then, since the analysis is restricted to radially symmetric apertures, the on-axis intensity is

$$I(0, 0; z) = \left|\int_0^{2\pi}\int_0^{\infty} t(\rho)\exp\left(\frac{i\pi z}{\lambda f^2}\rho^2\right)\rho d\rho d\phi\right|^2. \quad (10)$$

We now employ the change of variable $\rho = \rho(\zeta)$, previously introduced in Ref. 7, which transforms any two-dimensional radially symmetric aperture $t(\rho)$, defined for $0 \leq \rho \leq \rho_0$, into a modified one-dimensional pupil function $q(\zeta)$ that is different from zero only in the interval $-1/2 \leq \zeta \leq 1/2$; that is,

$$\left(\frac{\rho}{\rho_0}\right)^2 = \zeta + \frac{1}{2}. \quad (11)$$

Then the on-axis intensity becomes

$$I(0, 0; z) = \int\int_{-\infty}^{\infty} q\left(\zeta + \frac{\zeta'}{2}\right) q^*\left(\zeta - \frac{\zeta'}{2}\right) \times \exp\left(2\pi i \frac{z\rho_0^2}{2\lambda f^2}\zeta'\right) d\zeta d\zeta'. \quad (12)$$

By means of the WDF defined for one-dimensional functions, the SR can be rewritten as

$$S(z) = \int_{-\infty}^{\infty} W_q\left(\frac{\rho_0^2 z}{2\lambda f^2}, \zeta\right) d\zeta. \quad (13)$$

Therefore the SR for radially symmetric apertures can be obtained, for any out-of-focus plane, from a proper spatial-frequency projection of the WDF defined in the two-dimensional phase space that is associated with the transformed pupil function $q(\zeta)$.

As presented by us in Ref. 27, it is possible to obtain phase retardation functions that give rise to an increase in the image focal depth. To this end, the WDF of a certain aperture $t_0(\rho)$, which has an associated small depth of focus in the image space, is transformed through the change of variables in Eq. (11) into a one-dimensional aperture $q_0(\zeta)$ that is conveniently sheared by an amount α in the phase-space domain as follows:

$$W_q\left(\frac{z\rho_0^2}{2\lambda f^2}, \zeta\right) = W_{q_0}\left(\frac{z\rho_0^2}{2\lambda f^2} - \alpha\zeta, \zeta\right). \quad (14)$$

In this way, high-value portions of the original WDF translate toward previously low-value regions, thus producing a compensation effect that smooths the variation of the ζ slices of the WDF from which the axial intensity is achieved. Therefore when this new WDF is introduced into the expression of the SR [Eq. (13)], a more uniform on-axis image irradiance can be accomplished. In Ref. 27 we apply this method to a uniform aperture: $t_0(\rho) = \mathrm{circ}(\rho/\rho_0)$, which was selected because of its simplicity and energy considerations. The enhanced depth-of-focus pupil function that we obtained was

$$t(\rho) = \mathrm{circ}\left(\frac{\rho}{\rho_0}\right) \exp\left\{-i\pi\alpha\left[\left(\frac{\rho}{\rho_0}\right)^4 - \left(\frac{\rho}{\rho_0}\right)^2 + \frac{1}{4}\right]\right\}. \quad (15)$$

Through the change of variables introduced by Eq. (11), the original pupil function $t_0(\rho)$ can be expressed as $q_0(\zeta) = \mathrm{rect}(\zeta)$. Then, when we take into account Eq. (14), the WDF of the transformed pupil function $q(\zeta)$, which originates high focal depth, becomes

$$W_q\left(\frac{z\rho_0^2}{2\lambda f^2}; \zeta\right) = \int q_0\left(\zeta + \frac{\zeta'}{2}\right) q_0^*\left(\zeta - \frac{\zeta'}{2}\right) \times \exp(-i\pi 2\alpha\zeta\zeta') \exp\left(i\pi \frac{z\rho_0^2}{\lambda f^2}\zeta'\right) d\zeta'. \quad (16)$$

In order to characterize a certain amount of defocus Δz where the optical imaging system produces a rather uniform $S(z)$, we restrict the WDF as given by Eq. (16) to take the phase-space values that satisfy

$$\frac{z\rho_0^2}{2\lambda f^2} - \alpha\zeta = 0. \quad (17)$$

Inside this domain the WDF takes the form

$$W_q\left(\frac{z\rho_0^2}{2\lambda f^2}; \zeta = \frac{z\rho_0^2}{2\lambda\alpha f^2}\right) = \int \mathrm{rect}\left(\zeta + \frac{\zeta'}{2}\right) \mathrm{rect}\left(\zeta - \frac{\zeta'}{2}\right) d\zeta' = \begin{cases} -2\zeta + 1 & \zeta \geq 0 \\ 2\zeta + 1 & \zeta \leq 0 \end{cases}. \quad (18)$$

It can be seen that $W_q(z\rho_0^2/2\lambda f^2; \zeta = -z\rho_0^2/2\lambda\alpha f^2)$ is null for $\zeta \geq 1/2$. Hence for $\zeta = -1/2$ the maximum value of the depth of focus is obtained, i.e. $\Delta z = 2z_{\max}$, where

$$z_{\max} = \frac{\lambda f^2 \alpha}{\rho_0^2}. \quad (19)$$

In this way, if a pupil function with a certain depth of focus is required for a given optical system, it is possible to achieve it by a proper shear in the phase-space domain [by applying Eq. (19)]. It is important to note that this procedure is more general than the scheme expressed by Eqs. (14)–(19), as one can apply it to any other pupil function that has a symmetric WDF, in order to derive a new pupil function that takes into account the original pupil characteristics but with enhanced depth of focus.

Up to now, we have analyzed the behavior of the pupil function by taking into account the energy spread along the optical axis. For this reason, the SR provides an adequate criterion for evaluating the performance of the optical system. However, if we are interested in taking into account the degradation of the image resolution for increasing amounts of defocus, the OTF becomes a more relevant quality parameter. The OTF would allow a better understanding of the spatial-frequency performance of a given pupil function for different defocus values. In the following, we are interested in linking the OTF with the WDF that is associated with the pupil function, in a way that is similar to what we did with the SR. Therefore the OTF of a radially symmetric pupil with a transmittance $t(\rho)$ can be expressed as

$$\mathcal{H}(\nu; z) = \frac{\int_0^{\infty} |p(r'; z)|^2 J_0(2\pi\nu r') r' dr'}{\int_0^{\infty} |p(r'; z = 0)|^2 r' dr'}, \quad (20)$$

where $p(r'; z)$ is the PSF of the pupil with transmittance $t(\rho)$, J_0 is the Bessel function of zero order and the first kind, and ν means the modulus of the normalized spatial frequencies. To link this OTF with the WDF of $t(\rho)$, we first rewrite the squared modulus of the PSF as

$$|p(r';z)|^2 = \left|\int_0^\infty t(\rho)\exp\left(\frac{\pi i}{\lambda}\frac{z}{f^2}\rho^2\right)J_0\left(\frac{2\pi\rho r'}{\lambda f}\right)\rho\,d\rho\right|^2$$

$$= \int_0^\infty\int_0^\infty t(\rho)t^*(\rho')\exp\left\{\frac{\pi i}{\lambda}\frac{z}{f^2}[\rho^2-(\rho')^2]\right\} \times J_0\left(\frac{2\pi\rho r'}{\lambda f}\right)J_0\left(\frac{2\pi\rho' r'}{\lambda f}\right)\rho'\rho\,d\rho\,d\rho'. \quad (21)$$

Then, by employing the change of coordinates introduced in Eq. (11) and replacing Eq. (21) in the expression of the OTF, we obtain

$$\mathcal{H}(\nu;z) = \frac{1}{\int_0^\infty |p(r';0)|^2 r'\,dr'}\int_0^\infty\left\{\int_{-\infty}^\infty\int_{-\infty}^\infty q(\xi)q^*(\xi') \times J_0\left(\frac{2\pi\rho_0}{\lambda f}\sqrt{\xi+\frac{1}{2}}\,r'\right) \times J_0\left(\frac{2\pi\rho_0}{\lambda f}\sqrt{\xi'+\frac{1}{2}}\,r'\right) \times \exp\left[\frac{\pi i}{\lambda}\frac{{\rho_0}^2 z}{f^2}(\xi-\xi')\right]d\xi\,d\xi'\right\} \times J_0(2\pi\nu r')r'\,dr', \quad (22)$$

where $q(\xi)$ is the transformed one-dimensional pupil function. To link this expression with the WDF of the transformed pupil we rewrite Eq. (22) as

$$\mathcal{H}(\nu;z) = \frac{1}{\int_0^\infty |p(r')|^2 r'\,dr'}\int_0^\infty\left[\int_{-\infty}^\infty\int_{-\infty}^\infty q\left(\zeta+\frac{\zeta'}{2}\right) \times q^*\left(\zeta-\frac{\zeta'}{2}\right) \times J_0\left(\frac{2\pi\rho_0}{\lambda f}\sqrt{\zeta+\frac{\zeta'+1}{2}}\,r'\right) \times J_0\left(\frac{2\pi\rho_0}{\lambda f}\sqrt{\zeta-\frac{\zeta'-1}{2}}\,r'\right) \times \exp\left(\frac{\pi i}{\lambda}\frac{{\rho_0}^2 z}{f^2}\zeta'\right)d\zeta\,d\zeta'\right]J_0(2\pi\nu r')r'\,dr', \quad (23)$$

where $\zeta = (\xi+\xi')/2$; $\zeta' = \xi - \xi'$. From the definition of the WDF, we found that

$$\mathcal{H}(\nu;z) = \frac{\int_0^\infty\left[\int_{-\infty}^\infty W_{\hat{q}(\zeta;r')}\left(\frac{{\rho_0}^2 z}{2f^2\lambda};\zeta\right)d\zeta\right]J_0(2\pi\nu r')r'\,dr'}{\int_0^\infty\left[\int_{-\infty}^\infty W_{\hat{q}(\zeta,r')}\left(\frac{{\rho_0}^2 z}{2f^2\lambda};\zeta\right)d\zeta\right]r'\,dr'}, \quad (24)$$

where

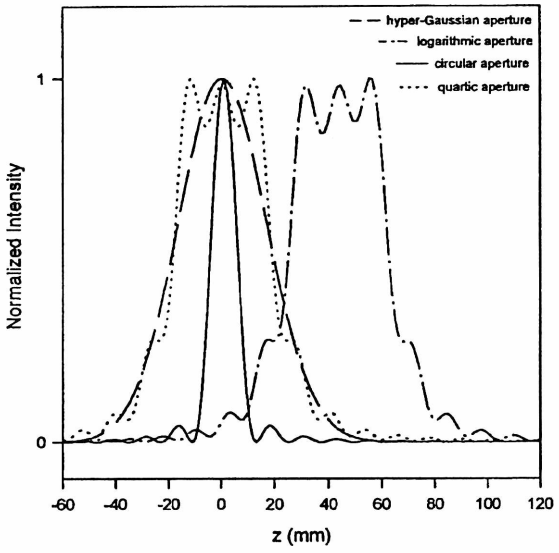

Fig. 1. Normalized intensity of the hyper-Gaussian pupil aperture, the logarithmic phase mask, the circular pupil function, and the quartic pupil function for extended depth of focus, Δz = 60 mm.

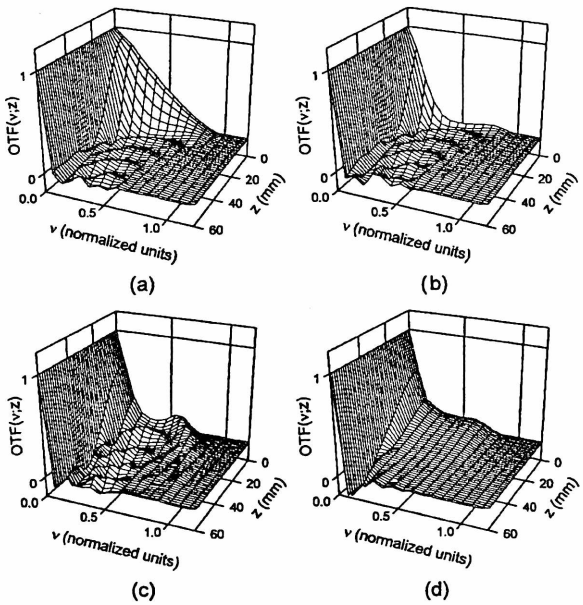

Fig. 2. Optical transfer function of (a) circular pupil function, (b) logarithmic pupil function, (c) quartic pupil function, (d) hyper-Gaussian pupil function for extended depth of focus, Δz = 60 mm.

$$\hat{q}(\zeta;r') = q(\zeta)J_0\left(\frac{2\pi\rho_0}{\lambda f}\sqrt{\zeta}\,r'\right). \quad (25)$$

Every WDF display corresponds to a different $\hat{q}(\zeta, r')$, as is expressed in Eq. (25), where $J_0(\zeta; r')$ acts as a window function for the transformed pupil function $q(\zeta)$, which is related to the original two-dimensional pupil function $t(\rho)$. Each WDF display shows the behavior of $\hat{q}(\zeta,\nu')$ for every z value and for each value of ν', so it would be necessary to evaluate an infinite number of WDF's, one

for each value of ν'. On the other hand, if we analyze the behavior of the transformed pupil function $\hat{q}(\zeta, \nu')$, we see that the zeros of the window function $J_0(\zeta; \nu')$ are fixed, so as ν' increases, ζ decreases; this means that for large ν', $\hat{q}(\zeta, \nu')$ can be approximated by $\hat{q}(\zeta, \nu') \approx q(0)J_0(2\pi\rho_0\sqrt{\zeta}\nu')$, and the contribution of the different WDF's to the OTF in Eq. (25) will be the same when ν' is large enough. In this way, the calculation of $\mathcal{H}(\nu; z)$ is greatly simplified.

It can be seen from Eq. (24) that, in a way similar to what was previously done for the case of the SR, the WDF associated with a one-dimensional modified pupil function provides information about the behavior of the OTF versus defocus. For diverse pupil functions $t(\rho)$, we obtain different $\hat{q}(\zeta, r_0')$, where r_0' is a fixed value of the variable r' that is selected according to the spatial-frequency band to be tested. Then the corresponding WDF's defined in the two-dimensional phase space $[x = (\rho_0{}^2 z)/(2f^2\lambda), \zeta]$ are obtained. In this way, the performances of the different pupil functions can be compared through the rate of variation of these displays along the x coordinate. The tolerance to defocus of the considered pupil functions is determined in a way similar to that for the analysis of $S(z)$, since there is a close resemblance between the ρ expressions in parentheses in Eqs. (13) and (24), which gives the SR.

4. RESULTS

To illustrate the present approach we analyze the SR and the OTF of different pupil functions. We compare the performance of four apertures: two phase pupil functions, the quartic phase plate introduced in Eq. (15), and the logarithmic phase mask,[11] given by

$$t(\rho) = \mathrm{circ}\left(\frac{\rho}{\rho_0}\right)\exp\left[\frac{i\pi\rho_0{}^2}{\lambda\,\delta z}\ln\left(f_0 + \frac{\delta z\rho^2}{\rho_0{}^2}\right)\right], \quad (26)$$

where δz is the focal depth; and two amplitude pupil functions, the hyperGaussian proposed by Ojeda-Castañeda *et al.*,[7]

$$t(\rho) = \mathrm{circ}\left(\frac{\rho}{\rho_0}\right)\exp\left\{-2\pi\gamma\left[\left(\frac{\rho}{\rho_0}\right)^2 - \frac{1}{2}\right]^2\right\}, \quad (27)$$

and the full circular pupil function. The normalized intensities for the four considered cases are shown in Fig. 1. The parameters of the pupil functions have been chosen to give similar depth of focus, and the lower tolerance to defocus of the full aperture can be seen. The corresponding OTF's for different values of z are shown in Fig. 2. For the circular and the logarithmic pupil functions, the OTF's dramatically decrease for out-of-focus planes, thus producing a serious degradation of their imaging capabili-

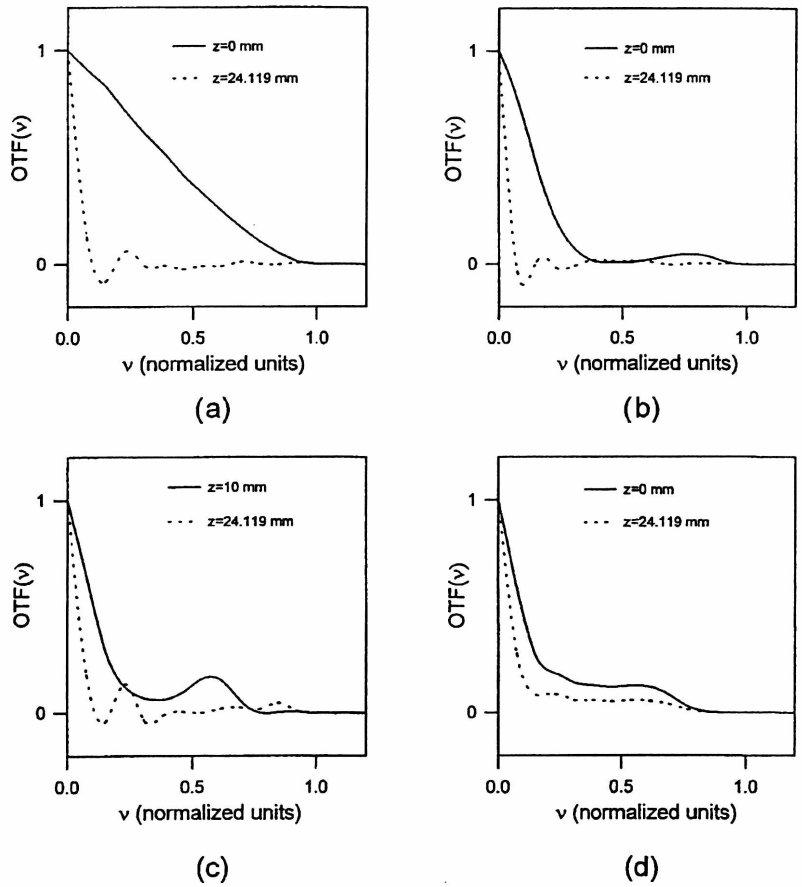

Fig. 3. Cross sections of the OTF of Fig. 2 for $z = 0$ mm and $z = 24.119$ mm. (a) Circular pupil function; some departure from the expected linear decrease (for $z = 0$ mm) due to the computational limitations in data sampling can be observed. (b) Logarithmic pupil function. (c) Quartic pupil function. (d) Hyper-Gaussian pupil function.

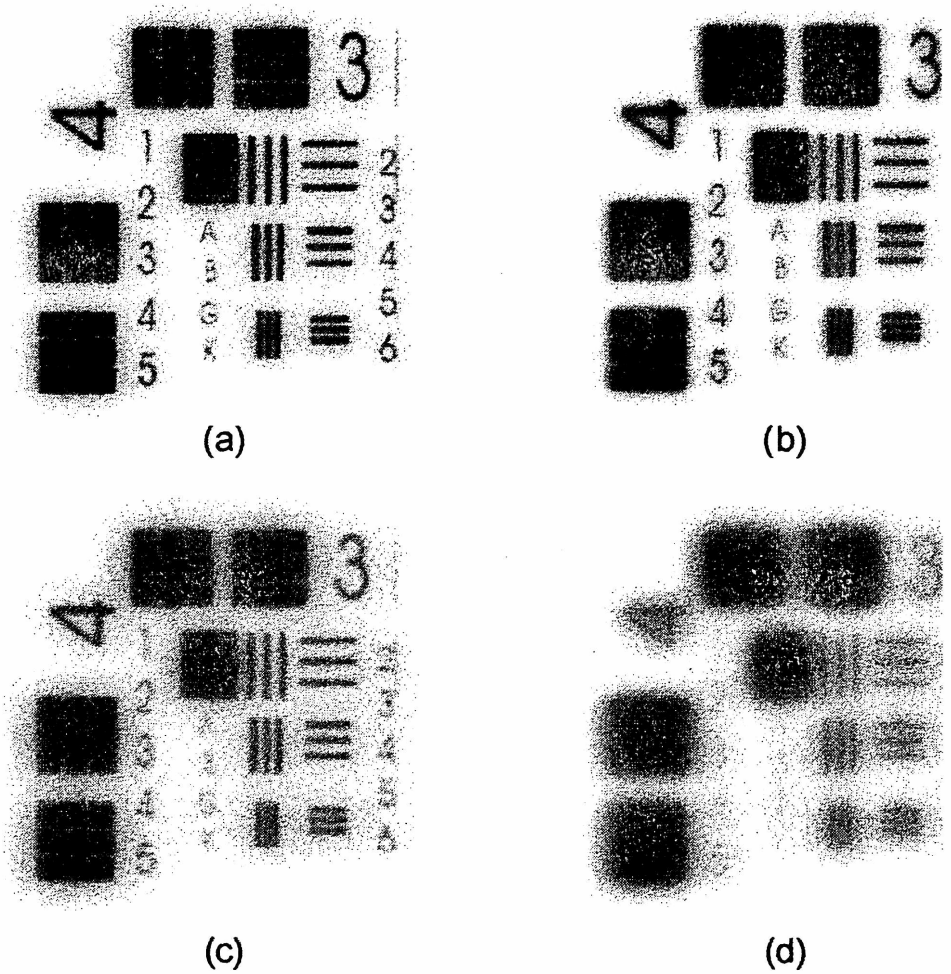

Fig. 4. Images of a test chart with (a) quartic pupil function for z = 10 mm, (b) hyper-Gaussian pupil function for z =0 mm, (c) quartic pupil function for z = 24.119 mm, (d) hyper-Gaussian pupil function for z = 24.119 mm.

ties. The OTF associated with the hyper-Gaussian pupil function shows a smoother decrease than the corresponding quartic aperture, but both of them produce better image quality than the circular and the logarithmic pupil functions. This fact can also be appreciated from Fig. 3. The OTF's associated with the quartic and hyper-Gaussian apertures for z = 0 mm and z = 24.199 mm show a better performance than for the other two pupils. For the quartic pupil function it can be seen that the cross section of the OTF presents spatial-frequency zones with better image resolution.

In Fig. 4 we compare the performance of the quartic and the hyper-gaussian pupil functions through the simulated images of a test chart for the best in-focus plane (z = 10 mm for the quartic pupil and z = 0 mm for the hyper-Gaussian pupil function), and for extreme defocus z = 24.119 mm. While for in-focus value the quartic and the hyper-Gaussian pupils present similar resolutions, for extreme depth of focus the quartic pupil has a better behavior than the hyper-Gaussian.

5. CONCLUSIONS

In the present paper we studied the SR and the OTF of different phase and amplitude pupil functions for varying defocus. We have linked these quality parameters with the WDF of these pupils. In this way, the SR could be visualized in a single phase-space representation of a one-dimensional modified pupil function. In another procedure, the OTF was analyzed by examination of the different WDF at various defocus distances. From these displays we obtained information directly about the behavior of the OTF criterion and the SR to analyze the image quality produced by four pupil functions with good tolerance to defocus. These relations between the quality parameters and the WDF have important implications in the design of optical imaging systems. Although the expression obtained for the OTF is more difficult to analyze than the equivalent expression for the SR, the present approach reduces calculation time.

Address correspondence to D. Zalvidea at the address

on the title page or by telephone, 54-221-4840280; fax, 54-221-4712771; or e-mail, dobrynaz@odin.ciop.unlp.edu.ar.

REFERENCES

1. L. M. Soroko, "Axicons and meso-optical imaging devices," in *Progress in Optics*, E. Wolf, ed. (Elsevier, New York, 1989), Vol. 27, pp. 109–160.
2. W. T. Welford, "Use of annular apertures to increase focal depth," J. Opt. Soc. Am. **50**, 749–753 (1960).
3. J. T. McCrickerd, "Coherent processing and depth of focus of annular aperture imagery," Appl. Opt. **10**, 2226–2230 (1971).
4. M. Mino and Y. Okano, "Improvement in the OTF of a defocused optical system through the use of shaded apertures," Appl. Opt. **10**, 2219–2225 (1971).
5. M. J. Yzuel and F. Calvo, "A study of the possibility of image optimization by apodization filters in optical systems of residual aberrations," Opt. Acta **26**, 1397–1406 (1979).
6. J. Ojeda-Castañeda, P. Andrés and A. Díaz, "Annular apodizers for low sensitivity to defocus and to spherical aberration," Opt. Lett. **11**, 487–489 (1986).
7. J. Ojeda-Castañeda, E. Tepichin, and A. Pons, "Apodization of annular apertures: Strehl ratio," Appl. Opt. **27**, 5140–5145 (1988).
8. J. Ojeda-Castañeda and L. R. Berriel-Valdós, "Zone-plate for arbitrarily high focal depth," Appl. Opt. **29**, 994–997 (1990).
9. G. Häusler, "A method to increase the depth of focus by two steps image processing," Opt. Commun. **6**, 38–42 (1972).
10. N. Davidson, A. A. Friesem, and E. Hasman, "Holographic axilens: high resolution and long focal depth," Opt. Lett. **16**, 523–525 (1991).
11. J. Sochacki, S. Bará, Z. Jaroszewicz, and A. Kołodziejczyck, "Phase retardation of uniform-intensity axilens," Opt. Lett. **17**, 7–9 (1992).
12. M. Born and E. Wolf, *Principles of Optics* (Pergamon, New York, 1989), pp. 460–464.
13. P. M. Duffieux, *L'intégrale de Fourier et ses Applications à l'Optique* (Imprimeries Oberthur, Rennes, France, 1946).
14. Lord Raleigh, "Investigations in optics with special reference to the spectroscopy," Philos. Mag. **8**, 261 (1879).
15. A. Maréchal, Ph.D. thesis (University of Paris, Paris, 1948).
16. H. H. Hopkins, "The aberration permissible in optical systems," Proc. Phys. Soc. London Sect. B **70**, 449–470 (1957).
17. H. H. Hopkins, "The use of diffraction-based criteria of image quality in automatic optical design," Opt. Acta **13**, 343–369 (1966).
18. M. J. Bastiaans, "The Wigner distribution function applied to optical signal and systems," Opt. Commun. **25**, 26–30 (1978).
19. M. J. Bastiaans, "The Wigner distribution function and Hamilton characteristics of a geometric-optical system," Opt. Commun. **30**, 321–326 (1979).
20. A. Papoulis, "Ambiguity function in Fourier optics," J. Opt. Soc. Am. **64**, 779–788 (1974).
21. K. H. Brenner, A. W. Lohmann, and J. Ojeda-Castañeda, "The ambiguity function as a polar display of the OTF," Opt. Commun. **44**, 323–326 (1983).
22. H. Bartelt, J. Ojeda-Castañeda, and E. E. Sicre, "Misfocus tolerance seen by simple inspection of the ambiguity function," Appl. Opt. **23**, 2693–2696 (1984).
23. J. Ojeda-Castañeda, P. Andrés, and E. Montes, "Phase-space representation of the Strehl ratio: ambiguity function," J. Opt. Soc. Am. A **4**, 313–317 (1987).
24. E. R. Dowsky, Jr., and W. Thomas Cathey, "Extended depth of field through wave-front coding," Appl. Opt. **34**, 1859–1866 (1995).
25. D. Zalvidea, M. Lehman, S. Granieri, and E. E. Sicre, "Analysis of the Strehl ratio using the Wigner distribution function," Opt. Commun. **118**, 207–214 (1995).
26. G. Saavedra, W. D. Furlan, E. Silvestre, and E. E. Sicre, "Analysis of the irradiance along different paths in the image space using the Wigner distribution function," Opt. Commun. **139**, 11–16 (1997).
27. D. Zalvidea and E. E. Sicre, "Phase pupil functions for focal depth enhancement derived from a Wigner distribution function," Appl. Opt. **37**, 3623–3627 (1998).
28. Z. Jaroszewicz and J. Morales, "Lens axicons: systems composed of a diverging aberrated lens and a perfect converging lens," J. Opt. Soc. Am. A **15**, 2383–2390 (1998).